AFRL-AFOSR-UK-TR-2015-0019

Development of Embedded Vascular Networks in FRP for Active/Passive Thermal Management

**Katarzyna Boba, Callum Heath, Mack McElroy,
Dr Andrew Lawrie, Dr Richard Trask, Prof Ian Bond**

**THE UNIVERSITY OF BRISTOL
ACCIS
SENATE HOUSE, TYNDALL AVENUE
BRISTOL, BS8 1TH
UNITED KINGDOM**

EOARD GRANT #FA8655-12-1-2144

Report Date: April 2015

Final Report from 30 September 2012 to 31 December 2014

**Air Force Research Laboratory
Air Force Office of Scientific Research
European Office of Aerospace Research and Development
Unit 4515, APO AE 09421-4515**

REPORT DOCUMENTATION PAGE

Form Approved OMB No. 0704-0188

1. REPORT DATE *(DD-MM-YYYY)*
1 April 2015

2. REPORT TYPE
Final Report

3. DATES COVERED *(From – To)*
30 September 2012 – 31 December 2014

4. TITLE AND SUBTITLE

Development of Embedded Vascular Networks in FRP for Active/Passive Thermal Management

5a. CONTRACT NUMBER

5b. GRANT NUMBER

FA8655-12-1-2144

5c. PROGRAM ELEMENT NUMBER

61102F

6. AUTHOR(S)

Katarzyna Boba, Callum Heath, Mack McElroy, Dr Andrew Lawrie, Dr Richard Trask, Prof Ian Bond

5d. PROJECT NUMBER

5d. TASK NUMBER

5e. WORK UNIT NUMBER

7. PERFORMING ORGANIZATION NAME(S) AND ADDRESS(ES)
THE UNIVERSITY OF BRISTOL
ACCIS
SENATE HOUSE, TYNDALL AVENUE
BRISTOL, BS8 1TH
UNITED KINGDOM

8. PERFORMING ORGANIZATION REPORT NUMBER

N/A

9. SPONSORING/MONITORING AGENCY NAME(S) AND ADDRESS(ES)

EOARD
Unit 4515
APO AE 09421-4515

10. SPONSOR/MONITOR'S ACRONYM(S)

AFRL/AFOSR/IOE (EOARD)

11. SPONSOR/MONITOR'S REPORT NUMBER(S)

AFRL-AFOSR-UK-TR-2015-0019

12. DISTRIBUTION/AVAILABILITY STATEMENT

Distribution A: Approved for public release; distribution is unlimited.

13. SUPPLEMENTARY NOTES

14. ABSTRACT

The increasing use of strong, lightweight composite materials in primary structural components within aerospace promises to substantially reduce aircraft non-payload weight, thereby improving fuel consumption and operating profitability. Weight reduction through use of polymer based composites for propulsion system components, however, can prove challenging due to the fact that the maximum operating temperature for a fiber-reinforced polymer composite is constrained by the glass transition temperature, Tg, typically in the range 100℃ - 200℃. This study sets out to investigate how the degradation of CFRP can be mitigated at raised temperature by applying a system of active cooling. Integration of vascular networks capable of cooling the host FRP component has been studied via a series of long term exposure, mechanical testing to measure the effect on interlaminar shear strength and fracture toughness. Results show that active cooling can realize significant reductions (50-70℃) in temperature compared to the operating environment (150℃), resulting in prolonged service performance. In parallel, a numerical model has been developed to evaluate performance to predict the temperature distribution in a thin flat plate that is subjected to a hot external air flow and is actively cooled by an internal vasculature and an external cool film. This thin plate test model offers a good first approximation to heat transfer properties for a gas turbine compressor blade. The vascular network topology in a structural component requires careful consideration to balance thermal efficiency between the vascular and film cooling effects. Experimental work is included which attempts to validate this numerical model, and indicates that this approach shows significant promise.

15. SUBJECT TERMS

EOARD, Materials, thermal management, vascular network

16. SECURITY CLASSIFICATION OF:			17. LIMITATION OF ABSTRACT	18, NUMBER OF PAGES	19a. NAME OF RESPONSIBLE PERSON
a. REPORT	b. ABSTRACT	c. THIS PAGE			Matthew Snyder
UNCLAS	UNCLAS	UNCLAS	SAR	18	19b. TELEPHONE NUMBER *(Include area code)* +44 (0)1895 616420

Project Title: **Development of Embedded Vascular Networks in FRP for Active/Passive Thermal Management**

Reference: **EOARD grant (FA8655-12-1-2144)**

Investigators: **Katarzyna Boba, Callum Heath, Mack McElroy, Dr Andrew Lawrie, Dr Richard Trask, Prof Ian Bond** (i.p.bond@bristol.ac.uk)

Final Report 1st April 2015

Abstract

The increasing use of strong, lightweight composite materials in primary structural components within aerospace promises to substantially reduce aircraft non-payload weight, thereby improving fuel consumption and operating profitability. Weight reduction through use of polymer based composites for propulsion system components, however, can prove challenging due to the fact that the maximum operating temperature for a fibre-reinforced polymer composite is constrained by the glass transition temperature, Tg, typically in the range 100˚C - 200˚C. This study sets out to investigate how the degradation of CFRP can be mitigated at raised temperature by applying a system of active cooling. Integration of vascular networks capable of cooling the host FRP component has been studied via a series of long term exposure, mechanical testing to measure the effect on interlaminar shear strength and fracture toughness. Results show that active cooling can realise significant reductions (50-70˚C) in temperature compared to the operating environment (150˚C), resulting in prolonged service performance.

In parallel, a numerical model has been developed to evaluate performance to predict the temperature distribution in a thin flat plate that is subjected to a hot external air flow and is actively cooled by an internal vasculature and an external cool film. This thin plate test model offers a good first approximation to heat transfer properties for a gas turbine compressor blade. The vascular network topology in a structural component requires careful consideration to balance thermal efficiency between the vascular and film cooling effects. Experimental work is included which attempts to validate this numerical model, and indicates that this approach shows significant promise.

1. Project Motivation and Objectives

The low density of fibre-reinforced polymer (FRP) composites, along with their high specific strength and stiffness, has driven the trend for their replacement of metallic materials in primary weight critical structures throughout the range of high performance structures. At the same time, thermal management has become a significant design consideration in modern structural materials and provides an opportunity for multifunctional materials incorporating active or passive cooling. It is envisaged that this approach could be used to adapt thermal signatures or allow extended operation in adverse environments.

The primary aim of this study is to develop and demonstrate thermal management of an FRP using integrated vascular networks to carry a heat transfer medium within typical aerospace-grade composite materials and using standard autoclave processing techniques.

The specific objectives are;

(a) to develop an embedded vascular network within a FRP, compatible with typical composite processing techniques,
(b) to integrate a functionality capable of effective manipulation of host structure thermal profile and explore the system requirements,
(c) to investigate the effectiveness of thermal management on preventing FRP degradation,
(d) to derive a modeling approach for effective cooling network operation in a composite component,
(e) to develop a proof-of-concept lab-scale demonstrator.

2. Outline of activities

2.1. Fabrication of vascular networks

Screening of alternative methods for creating the vascular networks in-situ was an initial part of the study, which resulted in three manufacturing techniques exploiting (i) hollow poly-lactic acid (PLA) fibres, (ii) PLA covered Nickel-Chrome (NiCr) wires and (iii) commercially available polytetrafluoroethylene (PTFE) covered NiCr wires. Each method bestowed various advantages and disadvantages for vascular network fabrication. After much experimentation, method (ii) has been successfully used to manufacture a simple branched network in a CFRP composite, as shown in Fig. 2.1 and Fig. 2.2.

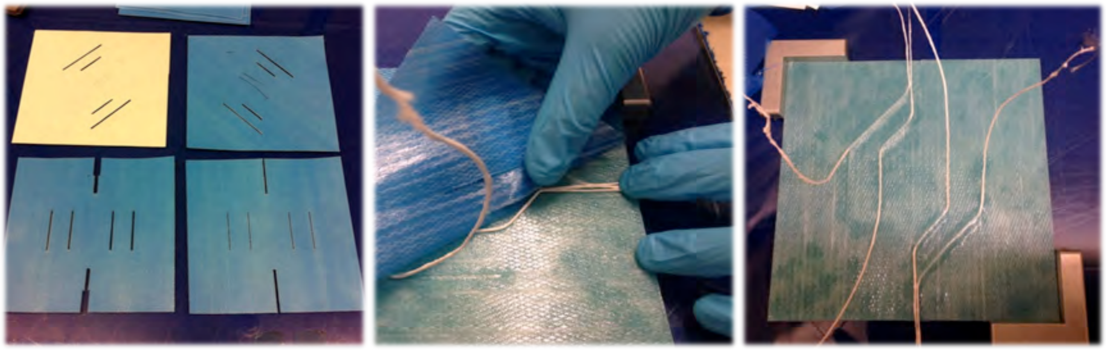

Fig 2.1. Hand layup of PLA coated NiCr wire into fibre direction cut-outs (SE70 Glass/epoxy prepreg)

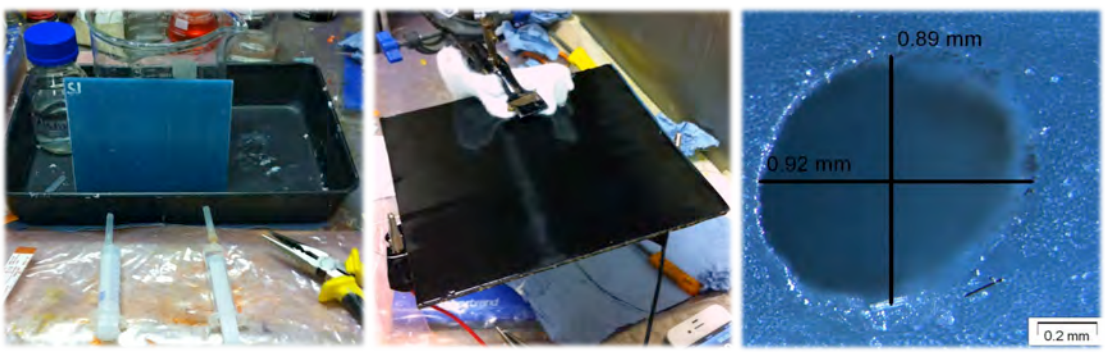

Fig 2.2. Softening PLA via resistive heating facilitates NiCr wire removal. Flush with solvent (CH3Cl) creating hollow vascules

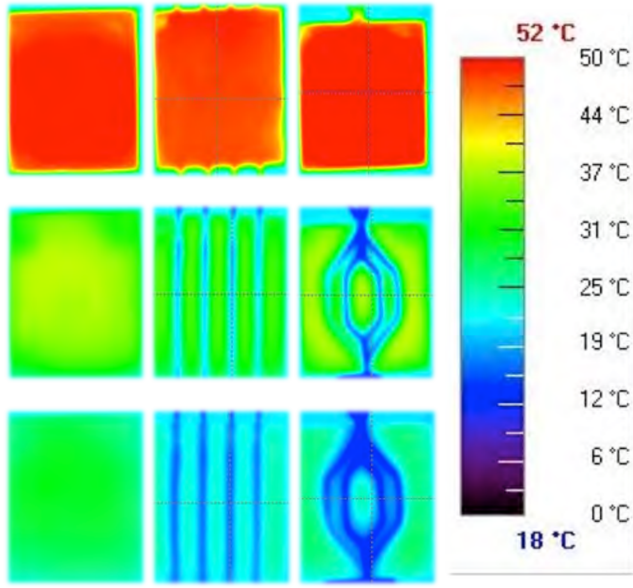

Fig. 2.3. Initial tests pumping water at 0˚C through Ø0.9 mm vascules at ≈30ml/min show different performance of network designs (left) baseline, (centre) *straight* and (right) *shape*, after (a) 0 minutes (top), (b) 2 minutes (middle), (c) 5 minutes (lower).

2.2. Preliminary thermal management trials

Three FRP unidirectional panels (16 plies, SE70 carbon/epoxy, Gurit UK) were manufactured, two with a vascular network design, see Fig. 2.3. Panel *straight*, was designed with four continuous straight vascules running along the length, whilst Panel *shape* had a network designed to allow single point entry/exit. Cooling to ambient was achieved from an initial panel temperature of 50˚C and 70˚C. Panel *shape* (branched) was found to yield a lower final temperature across the panel (after 5 minutes of cooling flow, iced water at 0˚C), but the thermal profile was uneven across the panel as shown in Fig 2.3. This test provided some insight into the manufacturability and cooling behaviour of vascular networks, and identified the scope for subsequent network optimization.

2.3. Suppression of thermal ageing in CFRP

Following the initial trials above, a study was established to investigate the suppression of thermal ageing in a thermoset CFRP (SE70 carbon/epoxy, Gurit, UK) using cooling via a simple embedded vascular network. CFRP test coupons have been thermally aged by exposure to 110˚C (10˚C below Tg) and 150˚C (30˚C above Tg), for up to 13 weeks to establish changes in mechanical performance using Short Beam Shear (SBS) specimens to measure Inter-Laminar Shear Strength (ILSS) and Double Cantilever Beam (DCB) specimens to test fracture toughness. These specimens were manufactured with and without the presence of active cooling via an embedded vasculature.

2.3.1 Experimental Methodology

DCB and SBS specimens were manufactured using low temperature cure unidirectional prepreg tape (SE70, carbon fibre/epoxy, Gurit UK), Fig. 2.4 and Fig. 2.5. To ensure compatibility, all specimens were manufactured with vascular channels in their structure.

For the DCB specimens, 18 plies of unidirectional material were used to give a nominal thickness of 3.6mm. A 19μm thickness PTFE release film was placed on the mid-plane and PTFE coated NiCr wires were inserted at specific locations as shown in Fig. 2.4. Following the manufacturers recommendations, a curing cycle of 50min at 110°C was applied, whereupon the wires were removed from the panels to produce the desired empty vascules. This short curing cycle was selected such that the resulting T_g of the cured laminate would be 126°C. Mode I DCB testing was performed according to the guidelines set out in ASTM D5528 at a 3mm/min loading rate. The crack tip was tracked using a high definition video camera with an accuracy of ±0.5mm for every 5mm of delamination growth.

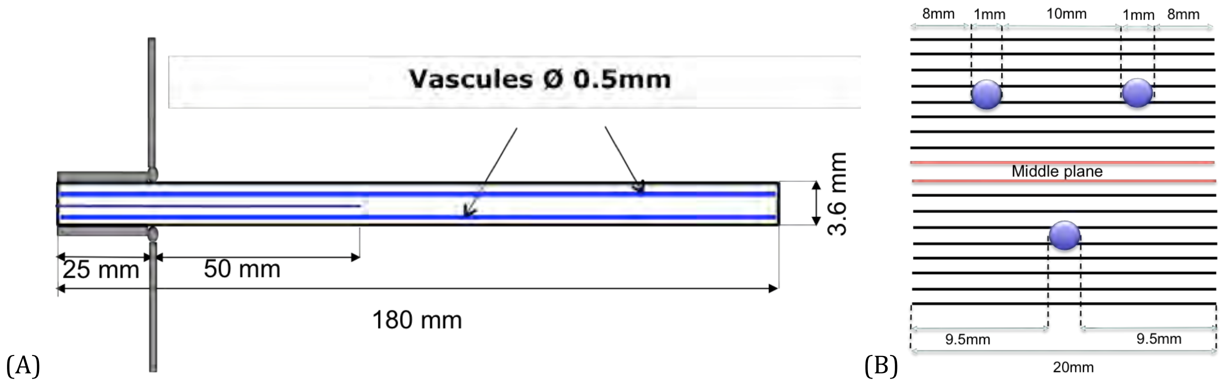

Fig. 2.4. Side (A) and cross-section (B) view of a DCB specimen with embedded vascular thermal management.

For the SBS specimens, 16 unidirectional plies were stacked to give a nominal thickness of 3.2mm. Specimens were machined to 25mm long and 10mm wide, to give a span to thickness ratio of 5. This sample size was chosen upon recommendation from [1] and ASTM D2344 in order to achieve the correct interlaminar shear failure mode. Considering the small size of the beams, they were prepared with only one vascule running along the mid-plane of the sample, as illustrated in Fig. 2.5a. Loading (in three-point bending) was applied at a rate of 1 mm/min using 20mm loading and 10mm supporting rollers. All SBS testing undertaken gave a valid interlaminar shear failure mode as shown in Fig. 2.5b.

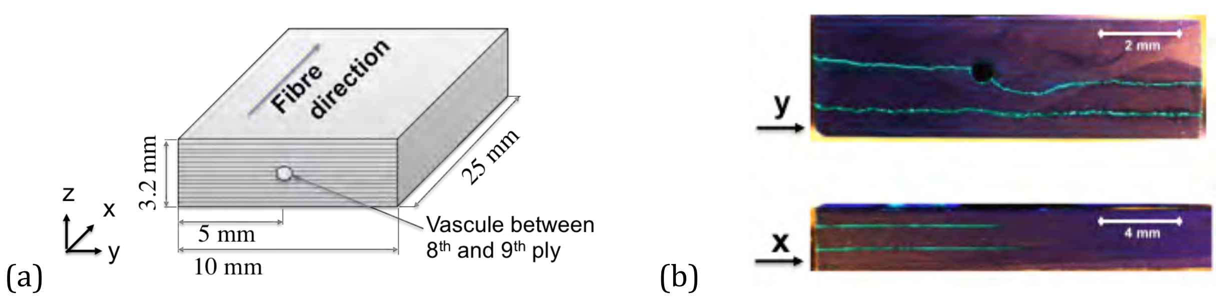

Fig. 2.5. (a) SBS sample dimensions and vascule location (b) Interlaminar shear failure mode in tested short beam shear specimen.

The DCB and SBS specimens were aged at a constant temperature in a standard convection oven and removed from the oven at intervals of approximately 170 hours (1 week) up to 2200 hours (13 weeks) for ageing at 110°C and 1200 hours (7 weeks) for ageing at 150°C. Following testing, the fractured surfaces of DCB specimens were examined using optical and scanning electron microscopy (SEM). The failure mode of the SBS specimens was investigated using optical microscopy. A UV fluorescent dye penetrant (Ardrox 9812) was applied to the damage site of the SBS specimens to enhance the visibility of the cracks.

Specimens subject to active cooling had hypodermic needles (25 gauge, shortened to 3mm length) inserted into the inlet and outlet of each channel, which enabled attachment of silicone tubing delivering cooling water to each specimen while in the oven. To secure the needles and avoid any leakage, the needles were bonded to specimens using cyanoacrylate glue, sealed with silicone adhesive. A mini peristaltic pump (Series 200, Williamson Manufacturing Company) was used to circulate ice-cold water (0°C) throughout the specimen at a rate of 10ml/min.

2.3.2 Cooling system design and testing

The active cooling system consists of a distilled water reservoir, a circulatory system (peristaltic pumps), a cooling unit (comprising a freezer (-18°C) with built in heat-exchanger), and a convection oven where up to six specimens can be aged/cooled simultaneously. The temperature of the oven and the specimens were monitored using thermocouples and recorded digitally. A schematic of the system is shown in Fig. 2.6.

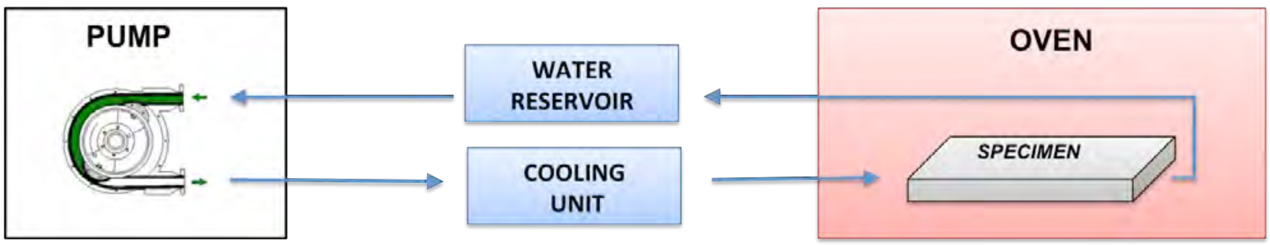

Fig. 2.6. Simplified schematic of the thermal ageing/active cooling system.

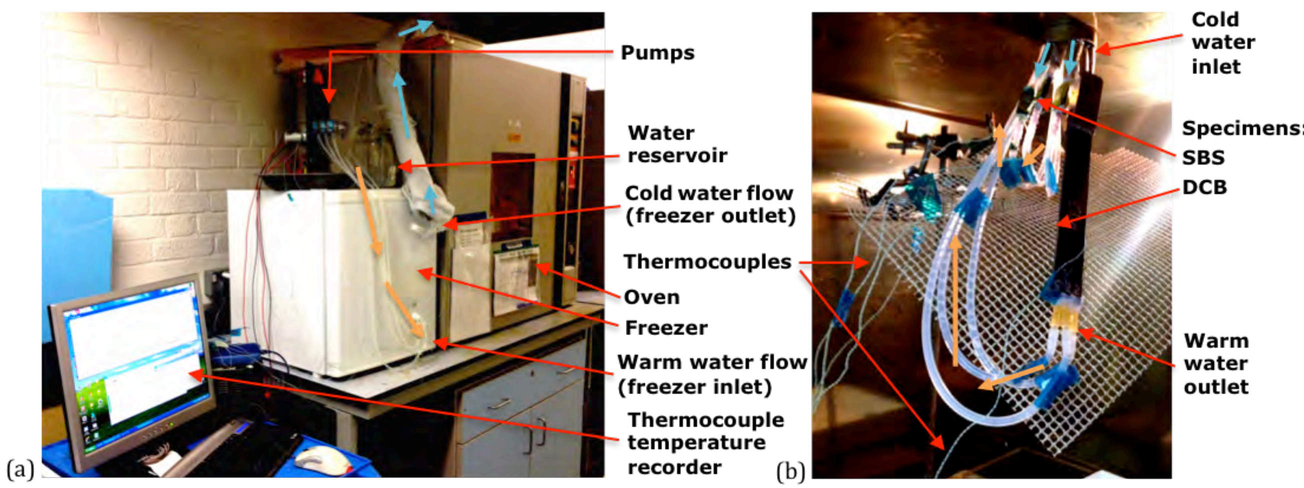

Fig. 2.7. (a) Cooling setup consisting of a computer recording the changes in temperature, pumps, water reservoir, cooling unit, an oven (b) specimens inside the oven, with attached tubing delivering cooling water and thermocouples reading the temperature of the specimen and the oven.

Initially, a series of tests using in-situ cooling were performed on both SBS and DCB specimens to establish the active cooling capability of the system. The specimens were placed into the oven through an opening in the top that allowed connection to the external cooling system. The cooling system is shown in Fig. 2.7a with the mounted specimens inside the oven shown in Fig. 2.7b. The temperature inside the oven was set to 110°C. After approximately 5 min of active cooling in the specimens, the temperature was recorded by the thermocouples located on the specimen as shown in Fig. 2.8. The thermocouples placed on the upper surface of the specimen (T_4) and close to the vascules (T_2, T_3) showed a reduction of approximately 50°C, as the specimen was reduced to 60°C. The thermocouple placed on the side of the specimen (T_1), which was furthest from the cooling effect of the vascule exhibited less reduction in temperature to 80°C. Active cooling was continued for one hour to identify any instabilities in the system, but no significant changes were noted and the specimen was successfully cooled throughout the duration of the experiment, Fig. 2.8. Further testing was undertaken at 150°C, and at 180°C. The latter saw a reduction to 100°C in the main body of the specimen (thermocouples T_2,

T_3. T_4), and 120°C further away from the vascules (thermocouple T_1), indicating that effective cooling could be achieved even at very high temperatures.

To investigate the inhibition of ageing by active cooling, SBS and DCB specimens were placed in the oven at 150°C. The samples were exposed to thermal ageing/active cooling for 24 hours, 48 hours, 170 hours (1 week) and 340 hours (2 weeks) before being mechanically tested.

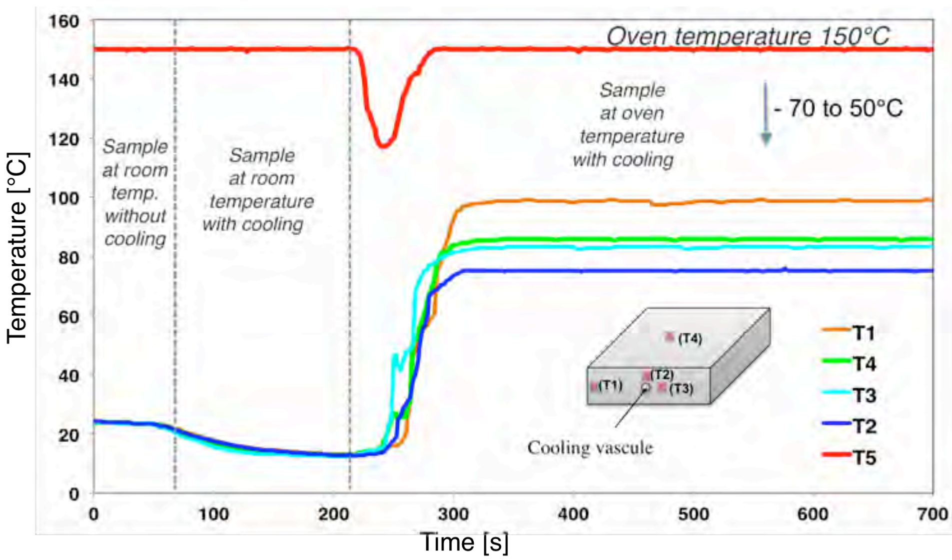

Fig. 2.8. Initial cooling results of SBS specimen at 150°C

2.3.3 Results of CFRP thermal ageing/active cooling

The interlaminar shear strength (ILSS) of pristine SBS specimens was calculated to be 83.2MPa (±1.2). With 1700 hours exposure to 110°C, no significant change in the shear strength of the material was measured. Only after 1850 hours was a significant reduction in the ILSS of the material observed, a decrease of 7% to 77.2 MPa (±1.0). The ILSS values were seen to further decrease, reaching 73.8MPa (±0.3) after 2200 hours, a loss of 12% compared to the reference value, as illustrated in Fig. 2.9. Since ILSS is dominated by the properties of the matrix and the fibre/matrix interphase, this indicates a degradation in the fibre/matrix interphase and possible defects developing in the matrix, resulting in decreased ILSS [2].
Specimens aged at 150°C saw a significant decrease in their ILSS after only one week of exposure, and were observed to continue to decrease up to 30% by week 8.
Specimens subjected to active cooling while exposed to 150°C were able to maintain comparable ILSS to specimens exposed to 110°C. More prolonged testing is needed to identify the extent of exposure whilst being actively cooled before a significant decrease in performance is observed.

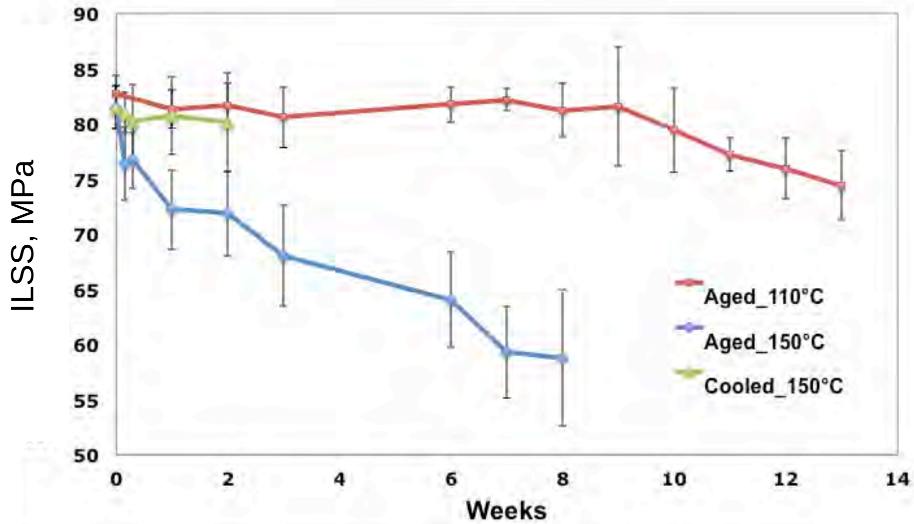

Fig. 2.9. ILSS resulting from isothermal ageing of SBS specimens exposed to 110°C, 150°C and actively cooled while exposed to 150°C.

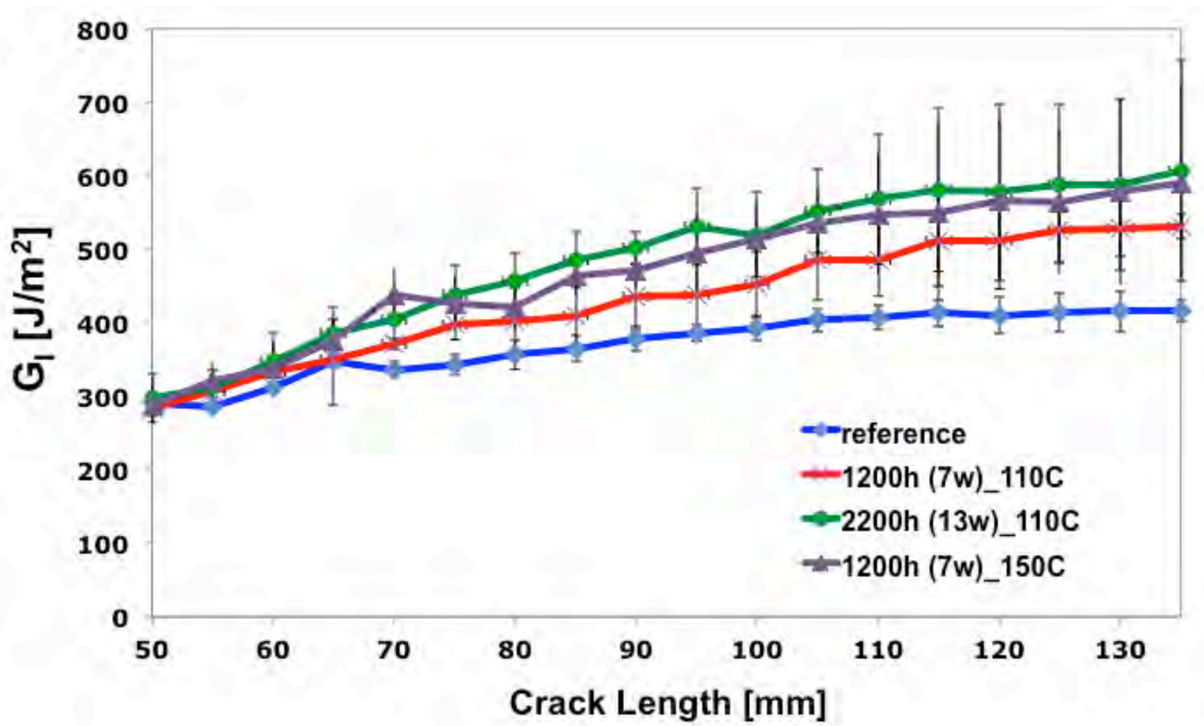

Fig. 2.10. Strain energy release rate (GIc) for thermally aged specimens. Fibre bridging was notable, particularly in specimens aged for 13 weeks at 110°C and 7 weeks at 150°C).

DCB test were undertaken in order to measure changes in mode I strain energy release rate, G_{IC} of the samples arising from thermal ageing. Fig. 2.10 shows the average GIc vs. crack length for reference specimens along with those aged for 7 weeks at 110°C and 150°C, and 13 weeks at 110°C. Whereas there seems to be negligible difference in initiation G_{ICi}, which remains at approximately 300 J/m^2, the steady state G_{IC} increases with the ageing duration, thus for the material aged for 13 weeks at 110°C, a value of G_{IC} 40% higher than the reference was observed. This indicates that a longer the temperature exposure duration, the more extensively the fibre/matrix interphase is affected leading to increased fibre bridging. This process is accelerated at higher temperature, especially when above the materials Tg. Fibre bridging is known to contribute significantly to the apparent propagation toughness, G_{ICp} value [3], [4]. This effect can be correlated with increased fibre pullout from the matrix during delamination and is associated with a degraded fibre/matrix interfacial strength.

It was observed that G_{ICp} (propagation) increases after 1000 hours of thermal ageing, however, no significant changes were noted in the value of G_{ICi} (initiation) for the whole exposure period. G_{ICi} is entirely matrix dependent, with little fibre involvement, whereas G_{ICp} involves fibre/matrix interface properties, as larger numbers of fibres are extracted at the fracture surface. This indicates that most of the thermally induced degradation occurs at the interphase connecting fibres with the matrix, causing reduced interfacial adhesion.

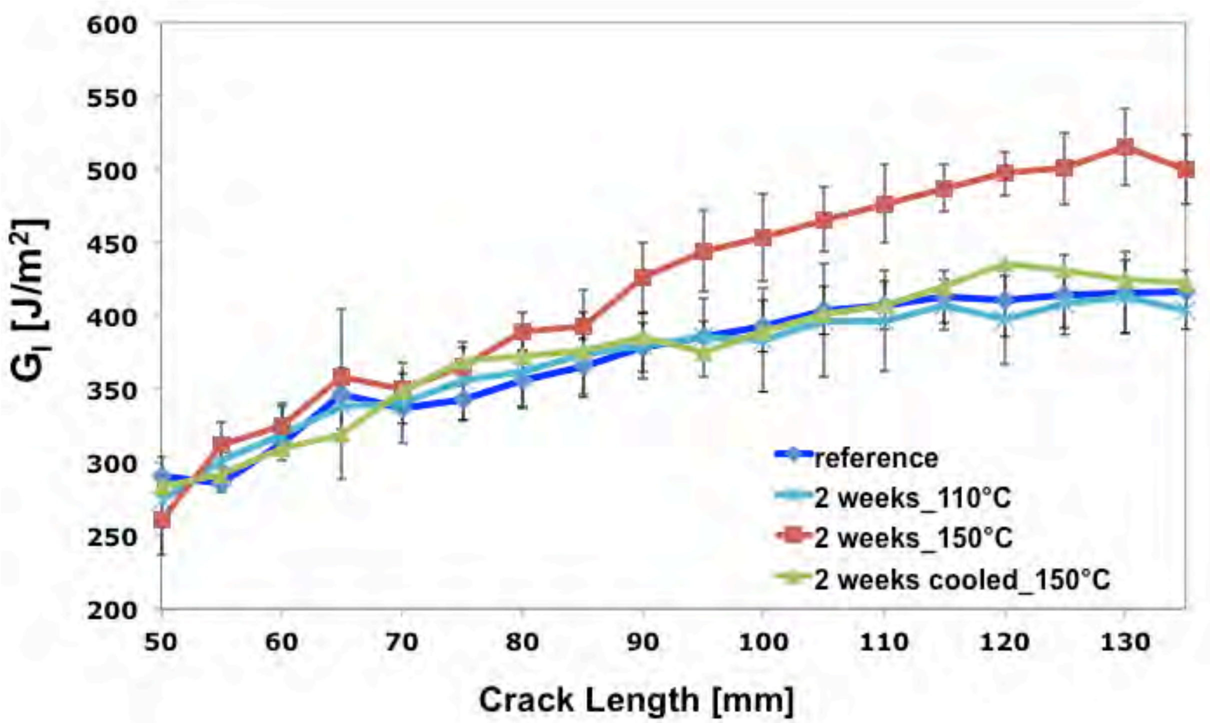

Fig. 2.11. Strain energy release rate (G_{IC}) after 2 weeks of thermal ageing at 110°C, 150°C and while actively cooled at 150°C. Apparent toughness increase attributed to fibre bridging, clearly visible for specimens aged at 150°C.

Changes in G_{IC} after two weeks of thermal ageing at 110°C, 150°C and while being actively cooled at 150°C, are shown in Fig. 2.11. The apparent toughness increase caused by fibre bridging is apparent for specimens aged at 150°C, whereas specimens which were actively cooled to a temperature below the Tg (<120°C) while in a 150°C environment, do not show any significant changes and are comparable to reference and specimens aged at 110°C.

2.3.4 Fractography

Scanning electron microscopy (SEM) was undertaken on the delamination surfaces of reference and thermally aged specimens, in the crack initiation (Fig. 2.12 (A)) and propagation regions (Fig. 12.2 (B)). The micrographs of the reference and aged samples taken in the initiation region do not reveal any noticeable differences, and predominantly matrix failure, little evidence of gross fibre pull-out. Conversely, the thermally aged specimens show abundant free fibres, detached from the matrix. This supports the findings from the mechanical testing, which suggests that the thermal degradation mainly occurred at the fibre/matrix interface.

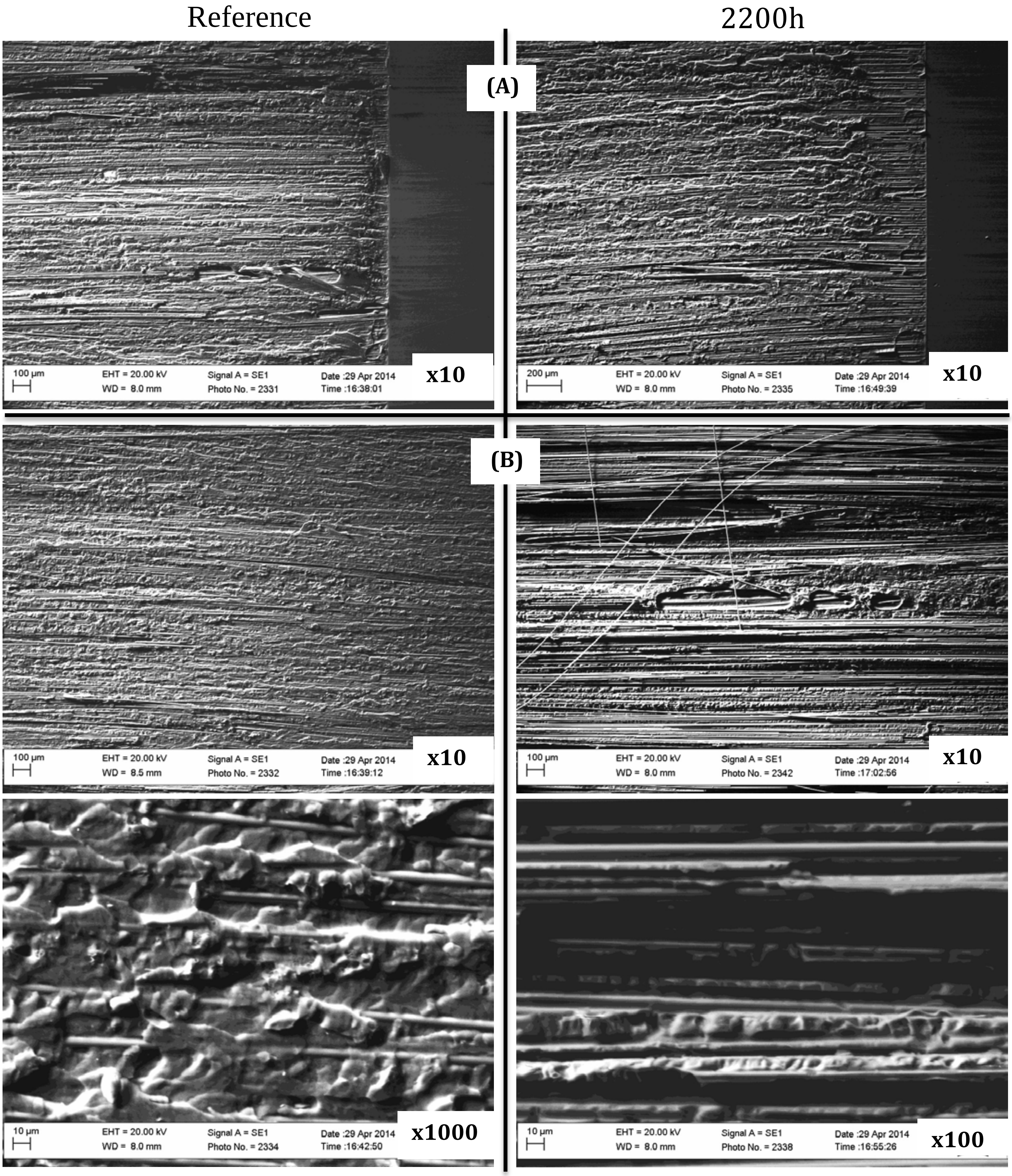

Fig. 2.12. SEM micrographs of fracture surfaces of reference and aged for 2200 hours DCB specimens: (A) at crack initiation region, (B) crack propagation region.

2.3.5 Summary of thermal ageing/active cooling in CFRP

Isothermal ageing has been undertaken on CFRP test coupons for 2200 hours (13 weeks) at 110°C and for 1200 hours (7 weeks) at 150°C on both SBS and DCB specimens incorporating embedded vascular channels.

For the SBS testing, results have shown significant decreases in ILSS; -7% after 1850 hours, -12% after 2200 hours for specimens aged at 110°C, and -30% following 1200 hours at 150°C.

For the DCB testing, significantly more fibre bridging was seen to occur in thermally aged samples, which resulted in an apparent increase in G_{ICp} values; +40% after 2200 hours ageing at 110°C and after 1200 hours ageing at 150°C.

Fracture surface analysis of DCB specimens using SEM indicated changes in the appearance, showing a larger number of fibres, detached from the matrix. These results indicate the detrimental effect on CFRP of extended exposure to raised temperature, even when close to or just below T_g. This work also highlighted that the most severely affected component as a result of thermal ageing is probably the fibre/matrix interface.

To investigate the feasibility of suppressing such degradation in material properties, a series of tests were performed with in-situ active cooling of both SBS and DCB specimens while exposed to a raised temperature environment. The specimens were exposed to either 110°C or 150°C, but with active cooling enabled (circulation of water (0°C) through the embedded vascules). The result was an apparent temperature reduction of approximately 50-70°C in the ageing specimens.

ILSS results for SBS specimens exposed to 150°C with active cooling were comparable to specimens aged at 110°C without cooling. Similarly, DCB testing has shown no significant difference in G_{IC} for specimens aged at 110°C and those which were actively cooled while exposed to 150°C. This indicates that the fibre/matrix interface has been somewhat protected by the active cooling approach.

An effective active cooling system has been developed and the results demonstrate that inhibition of isothermal ageing is achievable in a CFRP material with embedded vascular networks.

2.4 Active cooling - modelling & validation

2.4.1 Thermodynamic Modelling

While there are a small number of publicly available studies on the use of internal vascular cooling in polymer composite materials, none so far consider the role film cooling can play in improving thermal design. Lyall (2008) examined a stiffened composite panel for satellite electronics systems, containing fluidic microchannels for cooling [5]. This study was developed by Williams (2010) to include structural and thermal analysis [6]. Kozola (2010) explored the use of composite material for a fin with an internal vascular network using water or oil as the coolant. Additionally, a one-dimensional numerical heat transfer model of the fin surface was developed [7]. Quantifying the overall efficiency of a component containing an internal vascular network is an important question and in their work, Pierce and Phillips (2010, 2011) included a mechanical evaluation of a panel containing vascular cooling networks [8, 9].

To complement the materials characterisation work, a numerical model has been implemented in Matlab capable of determining the steady state temperature contour plot of a 2-D CFRP composite panel cooled simultaneously by an internal vascular network and an external cool air film, [simulating to a first approximation, a stator vane application in the compressor stage of a gas turbine]. This includes modeling the fluid mechanics and thermodynamics of the air flow within the vascules, using a compressible finite volume approach to simulate the internal vasculatory flow. Fourier's law is solved across the plate to estimate temperature distribution in thermal equilibrium. Film cooling is simulated based on a model derived from the classical solutions for viscous boundary layer growth. The thermal transport from the hot external gas stream towards the plate is estimated from empirical relations governing turbulent entrainment, treating temperature as a passive scalar. Geometric similarities mean that a thin plate test model offers a good first approximation to heat transfer properties for a gas turbine compressor blade.

In this study, the modelling activity was focused only on non-intersecting vascular topologies, but the proposed methodology is fully extendable to complex network topologies. Another restriction of the current model is that internal vascular flow remains laminar. Including turbulent flow in this study would introduce highly non-linear heat transfer behavior to the system and thus create a much more challenging problem.

Compressible Euler equations accounting for friction are discretised in one dimension with a first order flux-balance, and the mass flux is adjusted iteratively to satisfy a prescribed down-stream exit pressure given imposed upstream pressure and temperature boundary conditions.

The following equations are presented with regards to a single control volume (CV), with sub-scripts 1 and 2 representing the locations at the upstream and downstream faces, respectively. From mass conservation, the outlet velocity is given by;

$$v_2 = \frac{\dot{m} R_{sp} T_2}{P_2 A_{sec}} \qquad (1)$$

where A_{sec} is the cross sectional area of the tube, R_{sp} is the specific gas constant, m is the coolant mass flow rate, T is coolant temperature, and P is pressure. Conservation of energy in a steady flow is given by;

$$h_1 + \frac{v_1^2}{2} = h_2 + \frac{v_2^2}{2} + Q + W \qquad (2)$$

where h is enthalpy, Q is heat, and W is work due to friction (note that h, Q, and W are normalized by mass in this equation). Assuming laminar flow and using a Darcy friction factor, f, the change in pressure as a result of friction, ΔPf, is given as;

$$\Delta P_f = f \frac{dx}{2r} \frac{\rho v^2}{2} = \frac{64}{Re} \frac{dx}{2r} \frac{\rho v^2}{2} \qquad (3)$$

where, dx is the CV length, r is the control volume radius, v is coolant flow velocity, Re is the Reynolds number, and ρ is coolant density. A low-order approximation is made to the cell centre velocity used for estimating average wall friction, and is set equal to the inlet velocity v_1. Thus (2) can be written as;

$$Q = c_p(T_1 - T_2) + \frac{v_1^2 - v_2^2}{2} - A_{wall} \frac{8}{Re} \rho v_1^2 dx \qquad (4)$$

where A_{wall} is the surface area of a control volume. The rate of heat transfer, $\dot{Q}$, is obtained after multiplication of (4) by $\dot{m}$.

The heat transfer rate can alternatively be expressed as

$$\dot{Q} = A_{wall} U (T_1 - T_\infty) \qquad (5)$$

where T_∞ is external air temperature. Making the same low-order linearisation previously used to derive (4), inlet temperature T_1 is used to represent average temperature over a control volume. Multiplying (4) by $\dot{m}$ and equating with (5) yields a formulation of the energy equation suitable for sequential numerical evaluation of a single vessel from inlet to outlet given as;

$$\dot{m}\left[c_p(T_1 - T_2) + \frac{v_1^2 - v_2^2}{2} - A_{wall} \frac{8}{Re} \rho v_1^2 dx\right] = A_e U (T_1 - T_\infty) \qquad (6)$$

Equation (6) converges to the exact solution as CV length tends to zero and boundary conditions are iterated to consistency. The heat transfer coefficient, U, in (6) was shown by Pierce to vary weakly with mass flux [10]. However, it is shown later in the validation where U is treated as a constant, that the model performs well.

Using the form of the continuity equation shown by (1), the initial velocity, v_1, is obtained to use in (6). Conservation of momentum provides a third equation to the system, and is expressed as a Rayleigh condition;

$$P_1 A_{sec} + \dot{m} v_1 = P_2 A_{sec} + \dot{m} v_2 + \Delta P_f A_{sec} \quad (7)$$

The unknown variables T_2, P_2, and v_2 are found by solving (1), (6), and (7) simultaneously for each CV. Iteration proceeds until boundary conditions are satisfied and mass flux converges.

A two-dimensional numerical evaluation of Fourier's heat conduction law, $q_{cond} = -kA(dT/dx + dT/dy)$, predicts temperature $T(x, y)$ in the thin plate, where variations in the out-of-plane direction are considered negligible. Future versions of the model may be enhanced to be applicable to anisotropic heat flow by designating different heat transfer rates for the x and y directions based on the lay-up of a laminate.

Heat convection from the surrounding air occurring out-of-plane is accounted for using Newton's law of cooling, $q_{conv} = hA(T - T_\infty)$. An implicit second order finite difference scheme is formed from a standard 5-point stencil, in this instance on a regular grid. Source terms from CVs and external air temperature are linearly interpolated onto the regular grid. The proposed model of external film cooling from leading-edge apertures uses the well-known Blasius solution [10] to the boundary layer equations, $\delta(x) = 1.72\sqrt{\nu x/u}$, where ν is the kinematic viscosity, u is the free airstream velocity, and δ is the boundary layer thickness, to estimate the downstream growth of an insulating layer in the direction normal to the plate. A turbulent entrainment hypothesis is used to approximate transverse mixing of coolant air with the hot gas stream at a rate consistent with a spread angle of 12° [11]. An illustration of modelling assumptions with two internal vascules is shown in Fig. 2.13. The temperature of the aperture is assumed to be transferred to the insulating film, and the initial film thickness is set to match the aperture diameter.

The film air temperature varies along the air stream axis according to;

$$T = \left(\frac{A_x - A_o}{A_x}\right) T_\infty + \left(1 - \frac{A_x - A_o}{A_x}\right) T_{exit} \quad (8)$$

where A_o is the initial film section area, A_x is the film section area at a location along the free airstream defined by x, and T_{exit} is the coolant temperature at the aperture. Mixing was assumed to be sufficiently rapid relative to the temperature changes so that the film can be treated as having uniform temperature in a given cross-section.

When the geometry of a cool air film is determined on a panel, the resulting local film temperature replaces the external air temperature source term T_∞ in (6) in a new solution iteration. The updated T_∞ temperature distribution, in turn, then affects the temperature of the internal vascular coolant flow. Since the internal coolant flow supplies the cool film, an iterative loop is performed until the model solution converges as determined by a change in the standard deviation of the panel temperature from one iteration to the next of less than 1%.

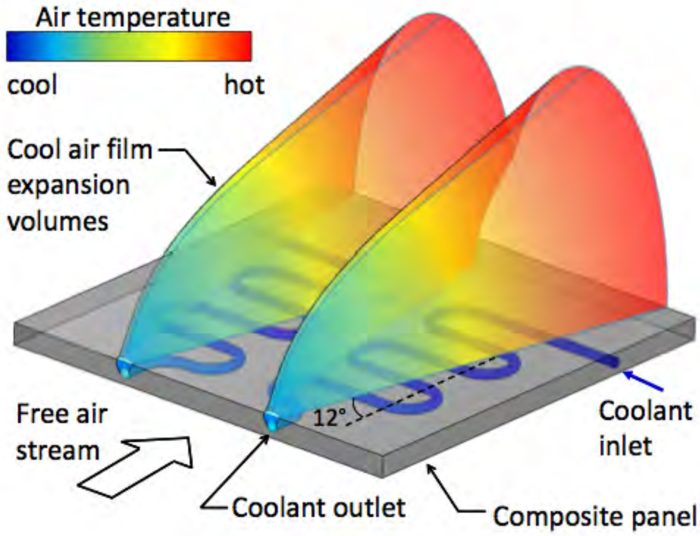

Fig. 2.13. Representative geometry and temperature variation of boundary layer cool air film.

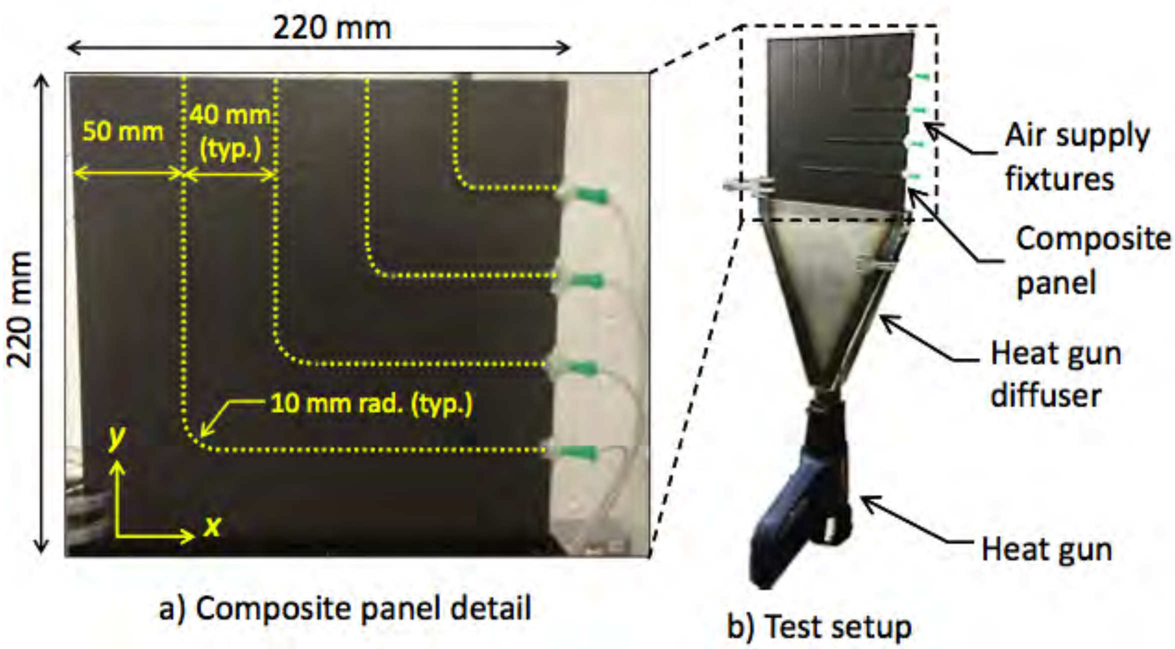

Fig. 2.14. CFRP composite panel with schematic of embedded cooling vasculature and connected air supply used for numerical model validation.

2.4.2 Experimental Validation

A flat CFRP panel (SE70, unidirectional carbon/epoxy, Gurit UK) containing a vascular network was fabricated to validate the numerical model described above (Fig. 2.14). As this testing was being used for model validation purposes, the vascules were well spaced in order to obtain internal coolant flows uninfluenced by nearby vascules. Additionally, in this configuration the overlap of contributions on panel temperature reduction from adjacent vascules is minimized. By isolating the flow behavior in each vascule and obtaining an exaggerated panel temperature variance in between vascules, the thermal behavior is somewhat simplified making the tests well suited for model validation.

The vasculature was connected to a compressed air supply and a hot gas stream was passed over the panel. Once in thermal equilibrium, thermal images were taken of the panel using a NEC Sanei Thermotracer Type TH9100MR IR camera and compared in detail to predictions from the numerical model whose output closely approximates panel surface temperature.

The panel was oven cured as recommended at 70°C for 16 hrs. The lay-up is $[\pm45, 90, 0_3]_s$ which results in a total panel thickness of 2.4 mm. Mechanical performance parameters such as laminate stiffness and strength were not a part of this study. Four centrally located 0° plies were cut into patterns such that a linear void would exist and define the geometry for a network of four vessels. During lay-up, 1.1 mm diameter PTFE coated steel wire was laid along four paths that would form the cooling vessels, using the technique outlined in section 2.1. Fittings were glued to the inlet points of each vessel to connect to an air supply. A photograph and overlaid schematic of the panel and vasculature network geometry is shown in Fig. 2.14a.

A hot gas stream from a Bosch heat gun was guided over the panel by a steel diffuser fabricated to match the panel geometry. Pressurized air at room temperature was supplied to a reservoir manifold, then distributed to the vessel inlets by pneumatic pipes. The heat gun, diffuser, and panel were assembled in a vertical orientation supported in place by clamps and test stands. A photograph of the test configuration is shown in Fig. 2.14b. On one side of the panel, six K-type thermocouples were attached to directly measure the air temperature at various locations on the panel. Vessel inlet flow temperature was measured using the thermal image of inlet flow pipes just outside the panel. Air flow velocity at the outlet of each vasculature was recorded using an anemometer, which is assumed to be minimally invasive to the flow. At the time of this report, experimentation that is specifically applicable to the boundary layer film cooling behavior in the model has not yet been performed.

Various external gas stream temperatures were used in testing, but the results above are for a heat gun setting of 140°C. To characterize the temperature distribution of heated air flowing across the exterior of the panel such that it can be easily used by the numerical model, thermocouple data was gathered at six panel locations and interpolated using an equation of the form, $y = a * exp(b/(x + c))$, in the streamwise direction and linearly in the cross-stream direction. Using vessel aperture anemometry data and the diameter of the aperture, mass flow rate was estimated for each of the four vessels as;

$$\dot{m} = \frac{v_2 P_2 A_{sec}}{R_{sp} T_2} \qquad (9)$$

where P_2 is set equal to the ambient room pressure (1 bar). Coolant pressure just upstream of the panel was determined as an input parameter for the thermodynamic model by a calibration process that involved iteratively varying the supply pressure until aperture coolant flow velocity and mass flow rate matched experimental data. Material properties used in the simulations are as follows:

- conductive heat transfer rate, k = 1.28 W/m K;
- overall heat transfer coefficient, U = 4.0 W/m^2 K (est.) [8, 9];
- convective heat transfer coefficient, h = 9.0 W/m^2 K [9];
- specific heat of air, c_p = 1005 J/kg K;
- kinematic viscosity of air at 20°C, ν = 1.568 m^2/2 x 10^6.

Fig's. 2.15(a) and 2.15(b) show a strong correlation between experiment and numerical predictions using a heat gun setting of 140°C and a calibrated inlet pressure of 1.2 bar. In addition to the visual temperature contour images, temperature profiles at cross-sections X-X and Y-Y are shown covering in detail the vessel inlet and outlet regions of the panel. The model's good correlation with the experiment suggests that it may be used as a reliable proxy for the thermodynamics of the physical system in similar panel designs.

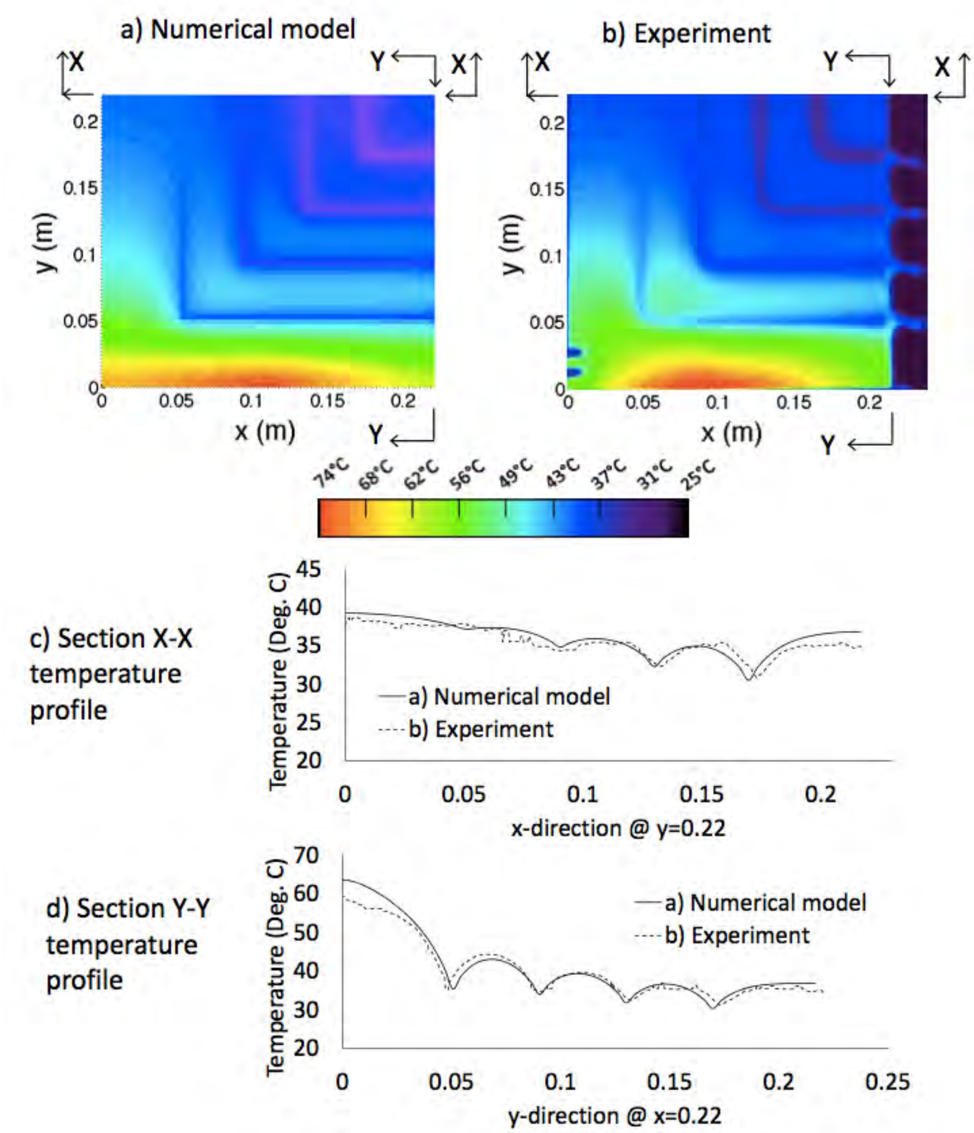

Fig. 2.15. Numerical model prediction versus experimental data from thermal testing. Heat gun set at 140°C. Air pressure inlet = 1.2 bar (abs). Cooling fluid temperature inlet = 29°C.

3.0 Summary

An investigation has been conducted on the performance of CFRP composite materials after exposure to raised temperature, envisaging their use as structural components in gas turbine engines. To mitigate the detrimental effects of temperature, an active cooling strategy has been demonstrated to ensure the material remains below it's glass transition temperature, T_g. Mechanical testing with and without active cooling via an embedded vascular network has highlighted the potential benefits of this approach on maintaining performance during exposure for prolonged periods at raised temperatures.

Alongside the materials characterisation, an experimentally validated simple numerical model was created that is capable of a thermal simulation of a thin composite panel actively cooled by an internal vascular network and an external boundary layer film. Using this model, an optimisation study can be readily applied to develop a cooling strategy for any component extending this model to a structure with more complex geometry and vasculature topology such as a cooled composite compressor blade in a gas turbine engine.

Following this initial feasibility study, further work may consider the following;

- effect of different lay-ups on conductive heat flow.
- influence of heat transfer coefficients as a function of mass flow rate.
- validation of the film cooling model.
- optimization or parametric studies of vasculature definition, i.e. network geometry, vascule radii, vascule density, etc.
- effect of vasculature on mechanical properties of panel
- full 3-D implementation of numerical model.

4.0 References

1. Cui, W., Wisnom, M.R., and Jones, M., Effect of specimen size on interlaminar shear strength of unidirectional carbon fibre-epoxy, Compos. Eng., vol. 4, no. 3, pp. 299–307, Jan. 1994.
2. Wolfrum, J., Eibl, S., and Lietch, L., Rapid evaluation of long-term thermal degradation of carbon fibre epoxy composites, Compos. Sci. Technol., vol. 69, no. 3–4, pp. 523–530, Mar. 2009.
3. Tsotsis, T. and Lee, S., Long-term thermo-oxidative aging in composite materials: failure mechanisms," Compos. Sci. Technol., vol. 3538, no. 97, pp. 355–368, 1998.
4. Johnson, W. and Mangalgiri, P, Investigation of fiber bridging in double cantilever beam specimens, J. Compos. Technol. Res., vol. 9(1), pp. 1–13, 1987.
5. Lyall, M.E. and Williams, A.D. and Arrit, B.S. and Taft, B.S. Experimental analysis of a biologically inspired thermal-structural satellite panel. 49th AIAA/ASME/ASCE/AHS/ASC Structures, Structural Dynamics, and Materials Conference, 7-10 April, Schaumburg, IL, 2008.
6. Williams, A.D. and Underwood, R.L. and Arritt, B.J. and Busch, G.T. and Taft, B.S. Biologically inspired multifunctional composite panel with integrated thermal control. 51st AIAA/ASME/ASCE/AHS/ASC Structures, Structural Dynamics, and Materials Conference, Orlando, FL, 2010.
7. Kozola, B.D. and Shipton, V.K. and Christensen, K.T. Characterization of active cooling and flow distribution in microvascular polymer. Journal of Intelligent Material Systems and Structures, 0, 1-10, 2010.
8. Pierce, M.R. Microvascular heat transfer analysis in carbon fiber composite materials. Master's Thesis, University of Dayton, 2010.
9. Phillips, D.M. and Pierce, M.R. and Baur, J.W. Mechanical and thermal analysis of microvascular networks in structural composite panels. Composites Part A, 42, 1609-1619, 2011.
10. Blasius, H. Grenzschichten in Flussigkeiten mit kleiner Reibung, Z. Math Physik, 56, 1-37, 1908.
11. Cushman-Roisin, B. Environmental Fluid Mechanics, John Wiley and Sons, 2014.